THE ASTROPHYSICAL JOURNAL, 505:523–528, 1998 October 1

TESTING COSMOLOGICAL VARIABILITY OF THE PROTON-TO-ELECTRON MASS RATIO USING THE SPECTRUM OF PKS 0528−250

ALEXANDER Y. POTEKHIN, ALEXANDER V. IVANCHIK, AND DMITRY A. VARSHALOVICH
Ioffe Physical-Technical Institute, 194021 St. Petersburg, Russia
KENNETH M. LANZETTA
Department of Physics and Astronomy, State University of New York at Stony Brook, Stony Brook, NY 11794-2100
JACK A. BALDWIN
Cerro Tololo Inter-American Observatory, Casilla 603, La Serena, Chile
GERARD M. WILLIGER
NASA Goddard Space Flight Center, Code 681, Greenbelt, MD 20771
AND
R. F. CARSWELL
Institute of Astronomy, Madingley Road, Cambridge CB3 0HA, England, UK
Received 1995 October 19; accepted 1998 April 23

ABSTRACT

Multidimensional cosmologies allow for variations of fundamental physical constants over the course of cosmological evolution, and different versions of the theories predict different time dependences. In particular, such variations could manifest themselves as changes of the proton-to-electron mass ratio $\mu = m_p/m_e$ over the period of $\sim 10^{10}$ yr since the moment of formation of high-redshift QSO spectra. Here we analyze a new high-resolution spectrum of the $z = 2.81080$ molecular hydrogen absorption system toward the QSO PKS 0528−250 to derive a new observational constraint to the time-averaged variation rate of the proton-to-electron mass ratio. We find $|\dot{\mu}/\mu| < 1.5 \times 10^{-14}$ yr^{-1}, which is much tighter than previously measured limits.

Subject headings: atomic data — cosmology: observations — elementary particles — quasars: absorption lines — quasars: individual (PKS 0528−250)

1. INTRODUCTION

The possibility of the variability of fundamental physical constants was first put forward by Dirac (1937) in the course of his discussion with Milne (1937). Later it was considered by Teller (1948), Gamow (1967), Dyson (1972), and other physicists. Interest in the problem has increased greatly during the last decade because of new developments in the Kaluza-Klein and supergravity models of the unification of all physical interactions. Chodos & Detweiler (1980), Freund (1982), Marciano (1984), and Maeda (1988) discussed the possibilities of including these multidimensional theories into the cosmological scenario of the expanding universe and found that the low-energy limits to the fundamental constants might vary over cosmological time. Variations of the coupling constants of strong and electroweak interactions might then cause the masses of elementary particles to change. Note that an increase of the proton mass by 0.08% would lead to transformation of protons into neutrons (by electron capture), resulting in destruction of atoms in the universe. As demonstrated by Kolb, Perry, & Walker (1986) and Barrow (1987), observational bounds on the time evolution of extraspatial dimensions in the Kaluza-Klein and superstring theories can be obtained from limits on possible variations of the coupling constants. Damour & Polyakov (1994) have developed a modern version of the string theory which assumes cosmological variations of the coupling constants and hadron-to-electron mass ratios. Therefore, the parameters of the theory can be restricted by testing cosmological changes of these ratios.

The present value of the proton-to-electron mass ratio is $\mu = 1836.152701(24)$ (Cohen & Taylor 1986). Obviously, any significant variation of this parameter over a small time interval is excluded, but such variation over the cosmological time $\sim 1.5 \times 10^{10}$ yr remains a possibility. This possibility can be checked by analyzing spectra of high-redshift QSOs.

The first analysis of this kind has been performed by Pagel (1977), who obtained a restriction $|\dot{\mu}/\mu| < 5 \times 10^{-11}$ yr^{-1} on the variation rate of μ by comparison of wavelengths of H I and heavy-ion absorption lines as proposed by Thompson (1975). This technique, however, could not provide a fully conclusive result, since heavy elements and hydrogen usually belong to different interstellar clouds moving with different radial velocities. In this paper we use another technique, based on an analysis of H_2 absorption lines only.

One object suitable for such analysis is the $z = 2.811$ absorption system toward PKS 0528−250, in which Levshakov & Varshalovich (1985) identified molecular hydrogen absorption lines based on a spectrum obtained by Morton et al. (1980). Foltz, Chaffee, & Black (1988) have presented a limit to possible variation of μ based on their observations of PKS 0528−250. Their analysis did not, however, take into account wavelength-to-mass sensitivity coefficients, so their result appeared to be not well grounded. Subsequently, the spectrum of Foltz et al. (1988) was reappraised by Varshalovich & Levshakov (1993), who obtained $|\Delta\mu/\mu| < 0.005$ at the redshift $z = 2.811$, and by Varshalovich & Potekhin (1995), who obtained $|\Delta\mu/\mu| < 0.002$ at the 2 σ significance level. (Here $\Delta\mu/\mu$ is the fractional variation of μ.) More recently, Cowie & Songaila (1995) used a new spectrum of PKS 0528−250 obtained with the Keck telescope to arrive at the 95% con-

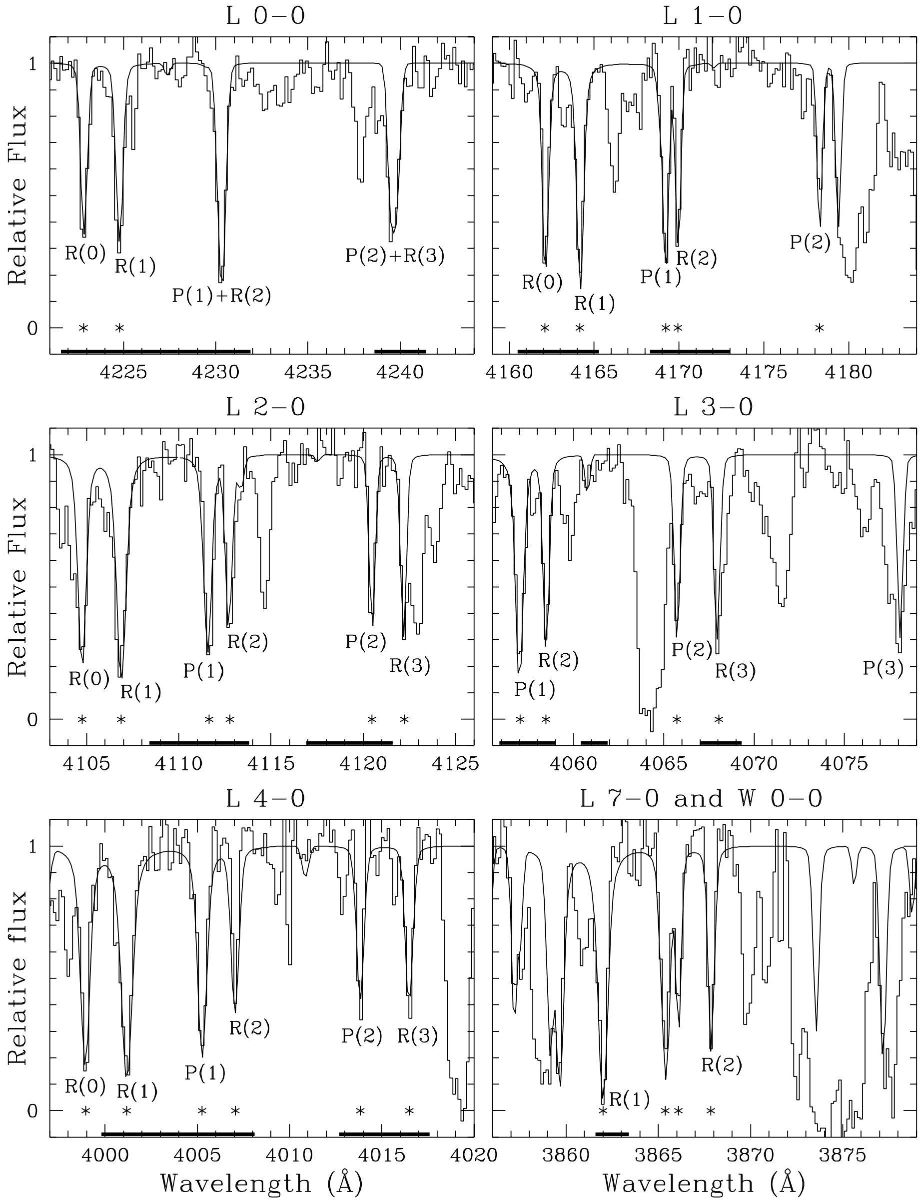

FIG. 1.—Selected parts of the spectrum PKS 0528−250 with absorption lines of H_2 molecules at the redshift $z = 2.81080$. The fit is superposed on the data. The most distinct absorption lines of the Lyman band are labeled on the plot. The thick bars along the horizontal axes mark the spectral intervals used in the fit (§ 4.1), and the asterisks mark the positions of individual lines listed in Table 2 and used in the independent analysis in § 4.2 (note that there are other spectral intervals and lines included in the analyses that belong to Lyman and Werner branches not shown in the figure).

fidence interval $-5.5 \times 10^{-4} < \Delta\mu/\mu < 7 \times 10^{-4}$.

Here we present a profile fitting analysis of a new high-resolution spectrum of PKS 0528−250 obtained in 1991 November with the Cerro Tololo Inter-American Observatory (CTIO) 4 m telescope. We have calculated the wavelength-to-mass sensitivity coefficients for a larger number of spectral lines and have employed them in the analysis, which yields the strongest observational constraint yet to possible μ-variation over the cosmological timescale (eq. [9] below).

2. OBSERVATIONS

Observations were obtained with the CTIO 4 m telescope in a series of exposures, typically of 2700 s duration, totaling 33,750 s duration. The CTIO Echelle Spectrograph with the Air Schmidt camera and Reticon CCD was used at a Cassegrain focus in order to obtain complete spectral coverage over the wavelength range $\lambda \approx 3465$–4905 Å. Observations of standard stars and of a Th-Ar comparison arc lamp were obtained at intervals throughout each night, and observations of a quartz lamp were obtained at the beginning or end of each night. For all observations, the slit was aligned to the parallactic angle.

Data reduction was performed following procedures similar to those described previously by Lanzetta et al. (1991). One-dimensional spectra were extracted from the two-dimensional images using an optimal extraction technique, and individual one-dimensional spectra were co-added using an optimal co-addition technique. Wavelength calibrations were determined from two-dimensional polynomial fits to spectral lines obtained in the Th-Ar comparison arc lamp observations. Continua were fitted to the one-dimensional spectra using an iterative spline-fitting technique.

TABLE 1

COEFFICIENTS Y_{mn} (in cm^{-1})

Coefficient	$X^1\Sigma_g^+$	$B^1\Sigma_u^+$	$C^1\Pi_u$
Y_{10}	2200.607	679.05	1221.89
Y_{20}	−121.336	−20.888	−69.524
Y_{30}	1.2194	1.0794	1.0968
Y_{40}	...	−0.1196	−0.0830
Y_{50}	...	0.00540	...
Y_{01}	60.8530	20.01541	31.3629
Y_{11}	−4.0622	−1.7768	−2.4971
Y_{21}	0.1154	0.2428	0.0592
Y_{31}	−0.0128	−0.0293	−0.00740
Y_{41}	...	0.00138	...
Y_{02}	−0.0942	−0.03250	−0.0446
Y_{12}	0.00685	0.005413	0.00185
Y_{22}	−0.0012	−0.0006867	...
Y_{32}	...	4.148×10^{-5}	...
Y_{03}	1.38×10^{-4}	...	...

The spectral resolution was measured from spectral lines obtained in the Th-Ar comparison arc lamp exposures. This is appropriate, because for all observations the seeing profile was larger than the slit width. The spectral resolution was found to be FWHM $\approx$ 21–24 km s^{-1} in the spectral intervals used for the analysis.

Figure 1 presents parts of the spectrum, with the fit superposed on the data, for several spectral intervals in which the H_2 absorption lines have been analyzed (for more detail, see Ćircovia et al. 1998).

3. SENSITIVITY COEFFICIENTS

The possibility of distinguishing between the cosmological redshift of the spectrum and wavelength shifts due to a variation of μ arises from the fact that the electronic, vibrational, and rotational energies of a molecule each undergo a different dependence on the reduced mass of the molecule. Hence, comparison of the wavelengths of various electronic-vibrational-rotational molecular absorption lines observed in the spectrum of a high-redshift quasar with corresponding molecular lines observed in the laboratory may reveal or limit the variation of μ with time.

If the value of μ at the early epoch z of the absorption spectrum formation were different from the contemporary one, then the ratio

$$\frac{(\lambda_i/\lambda_k)_z}{(\lambda_i/\lambda_k)_0} \simeq 1 + (K_i - K_k)\left(\frac{\Delta\mu}{\mu}\right) \tag{1}$$

would deviate from unity. Here

$$K_i = d \ln \lambda_i / d \ln \mu \tag{2}$$

is the coefficient that determines the sensitivity of the wavelength λ_i of the ith spectral line with respect to the variation of the mass ratio μ.

These coefficients were calculated previously by Varshalovich & Levshakov (1993) from the spectroscopic constants of the H_2 molecule using the Born-Oppenheimer approximation. Later, Varshalovich & Potekhin (1995) calculated K_i in another way, by comparison of the H_2 laboratory wavelengths with the corresponding wavelengths for D_2 and T_2 molecules (which only simulate the mass variation of the study) and HD molecules. Varshalovich & Potekhin (1995) also removed some inaccuracies from the table of Varshalovich & Levshakov (1993). The two ways of performing the calculation yielded very similar K_i values, which argues that both are correct.

For each electronic-vibrational-rotational band, a wavelength of a transition between two states with the vibrational and rotational quantum numbers v, J and v', J' can be presented as

$$\lambda = [\nu^u_{v'J'} - \nu^l_{v''J''}]^{-1} , \tag{3}$$

where ν is the level energy in cm^{-1} and the superscripts u and l stand for the upper and the lower level, respectively. For each of them,

$$\nu_{vJ} = \sum_{m,n} Y_{mn}(v + \tfrac{1}{2})^m [J(J+1)]^n . \tag{4}$$

We consider the Lyman bands (transitions $X^1\Sigma_g^+ \rightarrow B^1\Sigma_u^+$) and the Werner bands ($X^1\Sigma_g^+ \rightarrow C^1\Pi_u^+$) of the molecular H_2 spectrum. The parameters Y_{mn} for the three corresponding states are taken from Huber & Herzberg (1979). The coefficient Y_{00} is redefined so that the energy of each vibrational-rotational band is counted from the ground-state energy. For the state Π_u, the factor $J(J+1)$ in the terms with $n = 1$ of equation (4) has been replaced by $[J(J+1) - 1]$ in order to take into account the projection ($\Lambda^2 = 1$) of the electron orbital moment on the molecular axis.

From the Born-Oppenheimer approximation we conclude that the coefficients Y_{mn} are proportional to $\mu^{-n-m/2}$. Then the sensitivity coefficients K_i are easily obtained from equations (2)–(4):

$$K_{v'J'-v''J''} = \lambda_{v'J'-v''J''}(k^u_{v'J'} - k^l_{v''J''}) , \tag{5}$$

where

$$k_{vJ} = \sum_{m,n} Y_{mn}(v + \tfrac{1}{2})^m [J(J+1)]^n , \tag{6}$$

and the coefficients Y_{mn} are given in Table 1 (in cm^{-1}). For the state Π_u, the factor $J(J+1)$ in the terms with $n = 1$ has been replaced by $[J(J+1) - 1]$, as well as in equation (4).

4. RESULTS OF ANALYSIS

4.1. *Synthetic Spectrum Analysis*

We have applied a routine described previously by Lanzetta & Bowen (1992) to the spectrum. This routine performs a comparison of the synthetic and observed spectrum and finds an optimal solution to a parameterized model of a set of absorption profiles, simultaneously taking into account all observed spectral regions and transitions. Parameter estimates are determined by minimizing χ^2, and parameter uncertainties and correlations are determined by calculating the parameter covariance matrix at the resulting minimum.

A total of 59 H_2 transitions are incorporated into the χ^2 fit, and the absorption lines corresponding to these transitions occur across the linear, saturated, and damped parts of the curve of growth. The redshift, Doppler parameter, and column densities of the H_2 rotational levels $J'' = 0$ through $J'' = 7$ were adopted as free parameters. Wavelengths, oscillator strengths, and damping coefficients of the H_2 transitions were taken from Morton & Dinerstein (1976). According to Ćircovia et al. (1998), the total H_2 column density is $\log N(H_2) = 18.45 \pm 0.02$ and the Doppler parameter is $b = 3.23 \pm 0.11$ at the redshift

$$z = 2.8107998(24) . \tag{7}$$

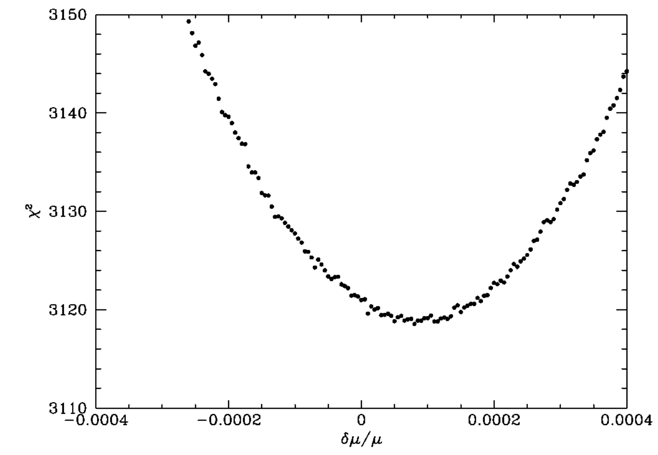

FIG. 2.—Best-fit (with respect to all other parameters of the problem) dependence of χ^2 on $\Delta\mu/\mu$. There are 1367 degrees of freedom in the χ^2 fitting analysis.

Full details of the reduction and analysis of the spectrum are described in a companion paper (Čircović et al. 1998), including the list of all spectral intervals and transitions used in the fit. These spectral intervals (shown in Fig. 1, *horizontal bars*) were chosen to embrace the anticipated positions of distinct and presumably unblended H_2 lines. We emphasize that although the choice of the window function is somewhat arbitrary, it should not entail systematic shifts of the parameter estimates. Note that there are H_2 lines present in the spectrum but not used in the fit. Some of them are seen in Figure 1 (for example, [L 1–0 P(2) and L 7–0 R(2)]). The wavelengths and strengths of these lines are perfectly reproduced by the synthetic spectrum. Furthermore, within the errors none of the model lines drops below the observed spectrum. This remarkable agreement between the measured and model synthetic spectrum confirms the reliability of the derived parameters.

A limit to the variation of the proton-to-electron inertial mass ratio was obtained by repeating the χ^2 synthetic spectrum-fitting analysis with an additional free parameter $\Delta\mu/\mu$. The dependence of χ^2 on this parameter is shown in Figure 2. The resulting parameter estimate and 1 σ uncertainty is

$$\Delta\mu/\mu = (8.3^{+6.6}_{-5.0}) \times 10^{-5} . \tag{8}$$

This result[1] indicates a value of $\Delta\mu/\mu$ that differs from 0 at the 1.6 σ level. The 2 σ confidence interval to $\Delta\mu/\mu$ is

$$-1.7 \times 10^{-5} < \Delta\mu/\mu < 2 \times 10^{-4} . \tag{9}$$

Assuming that the age of the universe is $\sim$15 Gyr, the redshift $z = 2.81080$ corresponds to the elapsed time of 13 Gyr (in the standard cosmological model with $\Omega = 1$). Therefore we arrive at the restriction

$$|\dot{\mu}/\mu| < 1.5 \times 10^{-14}\ \mathrm{yr}^{-1} \tag{10}$$

on the variation rate of μ, averaged over 87% of the lifetime of the universe.

4.2. *Profile Analysis of Separate Lines*

We have also analyzed the spectrum by another more traditional technique. This use of an alternative technique provides an independent check for the results of the above χ^2 analysis and enables a direct comparison with the previous results (Foltz et al. 1988; Varshalovich & Levshakov 1993; Varshalovich & Potekhin 1995; Cowie & Songaila 1995).

We have selected spectral lines of the Lyman and Werner bands which can be unambiguously fitted by a single Gaussian profile and a few lines whose decomposition in two contours is quite certain [such as L 1–0 P(1) and R(2) at $\lambda_z = 4170$ Å and L 7–0 P(1) and W 0–0 P(3) at $\lambda_z = 3866$ Å]. Since there are overlapping diffraction orders, we have selected them to work far from the order edges, and therefore the resolution in the analyzed regions was relatively high ($R > 10,000$) and uniform. The analyzed 50 transitions are listed in column (1) of Table 2 and marked in Figure 1 by asterisks. Only 26 of these 50 lines have been included in the analysis of the synthetic spectrum described in § 4.1, so the total number of H_2 wavelengths analyzed by both techniques amounts to 83. Thus, in this section we use not only an independent technique but also an independent choice of the spectral regions.

The rest frame wavelengths λ_0 adopted from Abgrall et al. (1993a, b) are given in column (2) of Table 2. The columns (3) and (4) of Table 2 present the optimal vacuum heliocentric position of the center of each observed profile (λ_z) and the estimated standard deviation (σ_λ). The values of λ_z and σ_λ have been provided simultaneously by the standard fitting procedure that minimized rms deviations between the fit and the data. Sensitivity coefficients K_i, calculated according to equations (5) and (6), are listed in column (5). The last column presents the redshift corresponding to each λ_z. These redshifts, z_i, are shown by crosses in Figure 3. In order to test the influence of possible uncertainty in λ_0, we have repeated the analysis using a set of wavelengths by Morton & Dinerstein (1976); the corresponding redshifts are shown in Figure 3 with open circles.

In the linear approximation, $z(K_i) = z + bK_i$ where $b = (1 + z)\Delta\mu/\mu$ and z is the cosmological redshift of the H_2 system. In order for the estimates of the regression parameters to be statistically independent, it is convenient to write

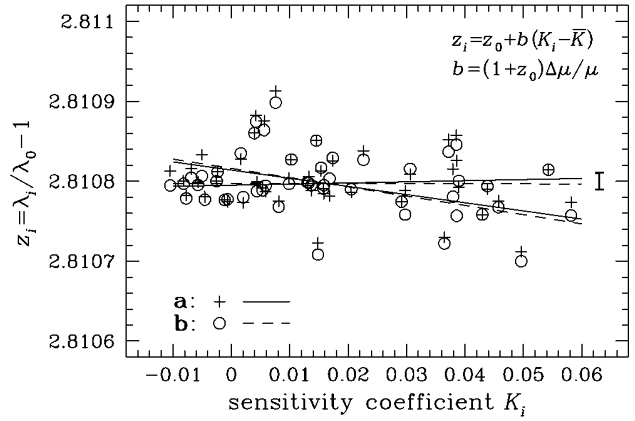

FIG. 3.—Relative deviations of the redshift values, inferred from an analysis of separate spectral features, plotted vs. sensitivity coefficients. The lines represent 2 σ deviations from the slope b of the best linear regression. The results based on the rest-frame wavelengths by (*a*) Morton & Dinerstein (1976) (*circles and dashes*) and (*b*) Abgrall et al. (1993a, b) (*crosses and solid lines*) are shown. The error bar to the right represents the ± 2 σ limit on z_0.

[1] The estimate (eq. [8]) was presented at the 17th Texas Symposium on Relativistic Astrophysics (Varshalovich & Levshakov 1996).

TABLE 2

H_2 Lines and Sensitivity Coefficients

Line	λ_0 (Å)	λ_z (Å)	σ_λ (Å)	K_λ	z_λ
L 0–0 $R(1)$	1108.633	4224.779	0.014	−0.00818	2.8107969
L 0–0 $R(0)$	1108.127	4222.830	0.010	−0.00772	2.8107782
L 1–0 $P(2)$	1096.438	4178.284	0.012	−0.00453	2.8107765
L 1–0 $R(2)$	1094.244	4169.945	0.012	−0.00252	2.8108000
L 1–0 $P(1)$	1094.052	4169.226	0.012	−0.00234	2.8108116
L 1–0 $R(1)$	1092.732	4164.157	0.008	−0.00113	2.8107761
L 1–0 $R(0)$	1092.195	4162.108	0.007	−0.00064	2.8107772
L 2–0 $R(3)$	1081.712	4122.218	0.011	0.00165	2.8108347
L 2–0 $P(2)$	1081.267	4120.463	0.015	0.00206	2.8107800
L 2–0 $R(2)$	1079.226	4112.779	0.012	0.00394	2.8108598
L 2–0 $P(1)$	1078.923	4111.648	0.008	0.00422	2.8108747
L 2–0 $R(1)$	1077.697	4106.879	0.016	0.00535	2.8107884
L 2–0 $R(0)$	1077.140	4104.751	0.080	0.00587	2.8107940
L 3–0 $R(3)$	1067.474	4068.050	0.095	0.00758	2.8108982
L 3–0 $P(2)$	1066.899	4065.712	0.117	0.00812	2.8107678
L 3–0 $R(2)$	1064.993	4058.479	0.020	0.00989	2.8107963
L 3–0 $P(1)$	1064.606	4057.029	0.019	0.01026	2.8108267
L 4–0 $R(3)$	1053.977	4016.490	0.012	0.01304	2.8107983
L 4–0 $P(2)$	1053.283	4013.838	0.010	0.01369	2.8107950
L 4–0 $R(2)$	1051.498	4007.062	0.010	0.01536	2.8108164
L 4–0 $P(1)$	1051.031	4005.259	0.008	0.01580	2.8107905
L 4–0 $R(1)$	1049.964	4001.183	0.030	0.01681	2.8108029
L 4–0 $R(0)$	1049.367	3998.954	0.014	0.01736	2.8108286
L 5–0 $R(4)$	1044.542	3980.460	0.031	0.01485	2.8107082
L 5–0 $P(3)$	1043.501	3976.557	0.005	0.01584	2.8107950
L 6–0 $P(3)$	1031.192	3929.652	0.050	0.02053	2.8107897
L 6–0 $R(3)$	1028.983	3921.287	0.010	0.02262	2.8108264
L 7–0 $R(2)$	1014.977	3867.848	0.007	0.02914	2.8107740
W 0–0 $P(3)$	1014.504	3866.085	0.014	−0.01045	2.8107942
L 7–0 $P(1)$	1014.326	3865.381	0.009	0.02976	2.8107576
L 7–0 $R(1)$	1013.436	3862.010	0.015	0.03062	2.8108155
W 0–0 $Q(2)$	1010.938	3852.498	0.010	−0.00686	2.8108040
W 0–0 $Q(1)$	1009.771	3848.034	0.011	−0.00570	2.8107949
W 0–0 $R(2)$	1009.023	3845.218	0.014	−0.00503	2.8108064
L 9–0 $R(2)$	993.547	3786.139	0.032	0.03647	2.8107220
L 9–0 $P(1)$	992.809	3783.448	0.023	0.03719	2.8108365
L 9–0 $R(1)$	992.013	3780.378	0.014	0.03796	2.8107804
L 9–0 $R(0)$	991.376	3777.961	0.042	0.03858	2.8107564
W 1–0 $R(3)$	987.447	3762.962	0.019	0.00439	2.8107874
W 1–0 $R(2)$	986.243	3758.449	0.018	0.00562	2.8108636
L 10–0 $P(2)$......	984.863	3753.172	0.009	0.03854	2.8108453
L 11–0 $P(3)$......	978.218	3727.786	0.011	0.03896	2.8108005
L 11–0 $R(2)$......	974.156	3712.273	0.013	0.04295	2.8107582
L 12–0 $R(3)$......	967.675	3687.606	0.029	0.04386	2.8107937
W 2–0 $R(3)$	966.778	3684.203	0.013	0.01324	2.8107977
W 2–0 $R(2)$	965.793	3680.493	0.009	0.01456	2.8108508
L 13–0 $P(3)$......	960.450	3660.059	0.017	0.04574	2.8107672
L 13–0 $R(2)$......	956.578	3645.243	0.010	0.04963	2.8106998
L 15–0 $P(3)$......	944.331	3598.670	0.042	0.05430	2.8108142
L 15–0 $R(2)$......	940.623	3584.501	0.029	0.05816	2.8107571

the regression in the form

$$z_i = z_0 + b(K_i - \bar{K}) , \tag{11}$$

where $\bar{K}$ is the mean value of K_i.

Given the typical values of $\sigma_\lambda \sim 0.02$ Å and $\lambda \sim 4000$ Å, one has a typical relative error of $\sigma_z \approx (\sigma_\lambda/\lambda)(1+z) \sim 2 \times 10^{-5}$ for an individual line. This estimate is only an intrinsic statistical error, and it does not include an error due to possible unresolved blends. For this reason, we have not relied on the estimated σ_λ values in our statistical analysis but calculated the 1 σ uncertainties from the actual scatter of the data (see also a discussion in Potekhin & Varshalovich 1994).

The estimated mean and slope parameters of the linear regression in equation (11), based on λ_0 by Morton & Dinerstein (1976), are $z_0 = 2.8107973(52)$ and $b = (-5.85 \pm 2.86) \times 10^{-4}$. Using the data of Abgrall et al. (1993a, b), we obtain $z_0 = 2.8108028(53)$ and $b = (-4.38 \pm 2.91) \times 10^{-4}$. The dashed and solid lines in Figure 3 correspond to the 2 σ deviations of b for the first and second sets of λ_0, respectively. The error bar to the right represents the 2 σ limit on z_0.

The latter estimate of b translates into

$$\Delta\mu/\mu = (-11.5 \pm 7.6) \times 10^{-5} . \tag{12}$$

When using the weights $\propto \sigma^{-2}{}_\lambda$, we obtain a similar estimate, $\Delta\mu/\mu = (-10.2 \pm 8.1) \times 10^{-5}$. Since the distribution of random errors caused by different sources (including possible blends) is not expected to be Gaussian, it may be worth using robust statistical techniques such as trimmed-mean regression analysis (e.g., Potekhin & Varshalovich 1994). We have applied the trimmed-mean technique of Ruppert & Carroll (1980) and found that at any trimming level up to 12% the estimate of b is closer to zero but has a larger estimated 1 σ error compared with the result of the standard least-squares analysis reported in equation (12). Thus we adopt equation (12) as the final result of this section.

Equation (12) has a larger statistical error compared with equation (8). Within 2 σ, both estimates are consistent with the null hypothesis of no variation of μ.

5. CONCLUSIONS

We have obtained a constraint to the variation rate of the proton-to-electron mass ratio μ. Two fitting procedures have been used, one of which simultaneously takes into account all observed spectral regions and transitions, while the other is applied to each spectral feature separately. The two techniques, applied to two different sets of spectral intervals, have resulted in similar upper bounds on $\Delta\mu/\mu$ at the level $\sim 2 \times 10^{-4}$. The obtained restriction on $\dot{\mu}/\mu$ (eq. [10]) is more stringent by an order of magnitude than the limit previously set by Varshalovich & Potekhin (1995), who used a spectrum with a lower spectral resolution. Moreover, it is much more restrictive than the estimate of Cowie & Songaila (1995), which is based on high-resolution Keck telescope observations. There are two reasons for the higher accuracy of the present estimate. First, our fitting procedure simultaneously takes into account all observed spectral regions and transitions. This is particularly important because many of the transitions are blended even at the spectral resolution of the spectrum used by Cowie & Songaila (1995). A separate analysis of spectral lines leads to larger statistical errors, as we have shown explicitly in § 4.2. Second, we include a larger number of transitions between excited states of the H_2 molecule (83 spectral lines, compared with 19 lines used by Cowie & Songaila), many of which have higher wavelength-to-mass sensitivity coefficients K_i. The larger interval of K_i values results in a higher sensitivity to possible mass-ratio deviations.

The method used here to determine the variation rate of μ could be less sensitive formally than one based on an analysis of relative abundances of chemical elements produced in primordial nucleosynthesis (Kolb et al. 1986). However, the latter method is very indirect because it depends on a physical model that includes a number of additional assumptions. Therefore, the present method seems to be more reliable.

Quite recently, Wiklind & Combes (1997) used a similar method (following Varshalovich & Potekhin 1996) in order to infer limits on time variability of masses of molecules CO, HCN, HNC, and the molecular ion HCO^+ from high-resolution radio observations of rotational lines in spectra of a few low-redshift ($z < 1$) quasars. The result reported in this paper constrains the mass of the H_2 molecule, and thus the proton mass, at much larger z. These constraints may be used for checking the multidimensional cosmological models that predict time dependences of fundamental physical constants. The described method of the calculation of the sensitivity coefficients can also be used for analyzing any other high-redshift molecular clouds that may be found in future observations.

A. Y. P., A. V. I., and D. A. V. acknowledge partial support from RBRF grant 96-02-16849 and ISF grant NUO 300. K. M. L. was supported by NASA grant NAGW-4433 and by a Career Development Award from the Dudley Observatory.

REFERENCES

Abgrall, H., Roueff, E., Launa, Y. F., Roncin, J. Y., & Subtil, J. L. 1993a, A&AS, 101, 273
———. 1993b, A&AS, 101, 323
Barrow, J. D. 1987, Phys. Rev. D, 35, 1805
Chodos, A., & Detweiler, S. 1980, Phys. Rev. D, 21, 2167
Ćircovia, M., Lanzetta, K. M., Baldwin, J., Williger, G., Carswell, R. F., Potekhin, A. Y., & Varshalovich, D. A. 1997, in preparation
Cohen, E. R., & Taylor, B. N. 1986, CODATA Bull., 63
Cowie, L. L., & Songaila, A. 1995, ApJ, 453, 596
Damour, T., & Polyakov, A. M. 1994, Nucl. Phys. B, 423, 532
Dirac, P. A. M. 1937, Nature, 139, 323
Dyson, F. J. 1972, in Aspects of Quantum Theory, ed. A. Salam & E. P. Wigner (Cambridge: Cambridge Univ. Press), 213
Foltz, C. B., Chaffee, F. H., & Black, J. H. 1988, ApJ, 324, 267
Freund, P. 1982, Nucl. Phys. B, 209, 146
Gamow, G. 1967, Phys. Rev. Lett., 19, 759
Huber, K. P., & Herzberg, G. 1979, Molecular Spectra and Molecular Structure. IV. Constants of Diatomic Molecules (Princeton: Van Nostrand)
Kolb, E. W., Perry, M. J., & Walker, T. P. 1986, Phys. Rev. D, 33, 869
Lanzetta, K. M., & Bowen, D. V. 1992, ApJ, 391, 48
Lanzetta, K. M., Wolfe, A. M., Turnshek, D. A., Lu, L., McMahon, R. G., & Hazard, C. 1991, ApJS, 77, 1
Levshakov, S. A., & Varshalovich, D. A. 1985, MNRAS, 212, 517
Maeda, K.-I. 1988, Mod. Phys. Lett., A3, 243
Marciano, W. J. 1984, Phys. Rev. Lett., 52, 489
Milne, E. 1937, Proc. R. Soc. London A, 158, 324
Morton, D. C., & Dinerstein, H. L. 1976, ApJ, 204, 1
Morton, D. C., Jian-sheng, C., Wright, A. E., Peterson, B. A., & Jaunsley, D. L. 1980, MNRAS, 193, 399
Pagel, B. 1977, MNRAS, 179, 81P
Potekhin, A. Y., & Varshalovich, D. A. 1994, A&AS, 104, 89
Ruppert, D., & Carroll, P. 1980, J. Am. Stat. Assoc., 75, 828
Teller, E. 1948, Phys. Rev., 73, 801
Thompson, R. 1975, Astron. Lett., 16, 3
Varshalovich, D. A., & Levshakov, S. A. 1993, J. Exp. Theor. Phys. Lett., 58, 237
Varshalovich, D. A., & Potekhin, A. Y. 1995, Space Sci. Rev., 74, 259
———. 1996, Astron. Lett., 22, 1
Wiklind, T., & Combes, F. 1997, A&A, 328, 48